



OPEN

SUBJECT AREAS:

POLYMERS

STRUCTURE OF SOLIDS AND
LIQUIDS

Received

22 August 2014

Accepted

28 November 2014

Published

16 December 2014

Correspondence and requests for materials should be addressed to L.B.L. (lbli@ustc.edu.cn) or H.Y.L. (hyliang@ustc.edu.cn)

Toughening mystery of natural rubber deciphered by double network incorporating hierarchical structures

Weiming Zhou¹, Xiangyang Li¹, Jie Lu¹, Ningdong Huang¹, Liang Chen¹, Zeming Qi¹, Liangbin Li¹ & Haiyi Liang²

¹National Synchrotron Radiation Lab and College of Nuclear Science and Technology, CAS Key Laboratory of Soft Matter Chemistry, University of Science and Technology of China, Hefei, China, ²Department of Modern Mechanics, University of Science and Technology of China, Hefei, China.

As an indispensable material for modern society, natural rubber possesses peerless mechanical properties such as strength and toughness over its artificial analogues, which remains a mystery. Intensive experimental and theoretical investigations have revealed the self-enhancement of natural rubber due to strain-induced crystallization. However a rigorous model on the self-enhancement, elucidating natural rubber's extraordinary mechanical properties, is obscured by deficient understanding of the local hierarchical structure under strain. With spatially resolved synchrotron radiation micro-beam scanning X-ray diffraction we discover weak oscillation in distributions of strain-induced crystallinity around crack tip for stretched natural rubber film, demonstrating a soft-hard double network structure. The fracture energy enhancement factor obtained by utilizing the double network model indicates an enhancement of toughness by 3 orders. It's proposed that upon stretching spontaneously developed double network structures integrating hierarchy at multi length-scale in natural rubber play an essential role in its remarkable mechanical performance.

Natural rubber is remarkable for its hyperelasticity, low hysteresis, and high fracture toughness, with indispensable applications in tires for aircrafts or heavy trucks, medical instruments, seismic isolation systems and *etc.*, which occupies about half of total rubber consumption with annual volume more than 10 million tons globally. The main supply of natural rubber is limited in Southeast Asia and attempts for synthetic rubber began as early as the dawn of rubber industry. However, even with the same *cis*-polyisoprene molecule, the artificial analogues typically exhibit 70–80% of elastic modulus, tensile strength and tearing resistance of natural rubber. The peerless mechanical strength for natural rubber has been attributed to its capacity of strain induced crystallization¹, a merit of natural rubber rooted in its perfect (100%) stereo-regularity of constituent molecules^{2,3}. Interestingly, it was found recently that lightly cross-linked natural rubber own outstanding shape memory properties and superior capability to in-situ sense and even remember solvent vapor concentrations due to the ability of strain induced crystallization^{4–8}. However, despite intensive theoretical^{2,9–11} and experimental^{12–19} investigations on the self-enhancement mechanism have been performed since 1925, the mechanism of strain-induced crystallization has not been elucidated very well. Class view proposes that these lamellae generated by crystallization act as the role of in-situ hard fillers embedded in soft amorphous matrix and physical cross-link in stretched natural rubber, increasing the Young's moduli and fracture toughness^{16,19–23}. The hierarchical structure is reminiscent of nacre²⁴, spider silk^{25,26}, bone^{27,28} and shish-kebab²⁹, which possess extraordinary mechanical strength and toughness due to the ability of dispersing stress concentration via concerted shear deformations among hard and soft components³⁰. Similar toughening mechanism is also assumed pertinent to the mechanical enhancement of natural rubber^{20,21}. However, the detailed mechanism and constitutive model of this crystallization-induced reinforcement remains unresolved yet, which may be the key to bridge the gap between natural and synthetic rubbers since the latter usually exhibit worse crystallinity due to imperfect stereo-regularity.

One critical assessment of the aforementioned toughening mechanism is to exam the fracture behaviors of stretched natural rubber films with crack. The induced hierarchical structure around the crack tip may modify the materials' properties and subsequently influence the crack resistance. Decreasing trend of the local crystallinity away from crack tip was obtained by using wide angle X-ray diffraction (WAXD)³¹. However, the low spatial resolution or small mapping area in these antecedent studies may smooth out or overlook the detailed structural

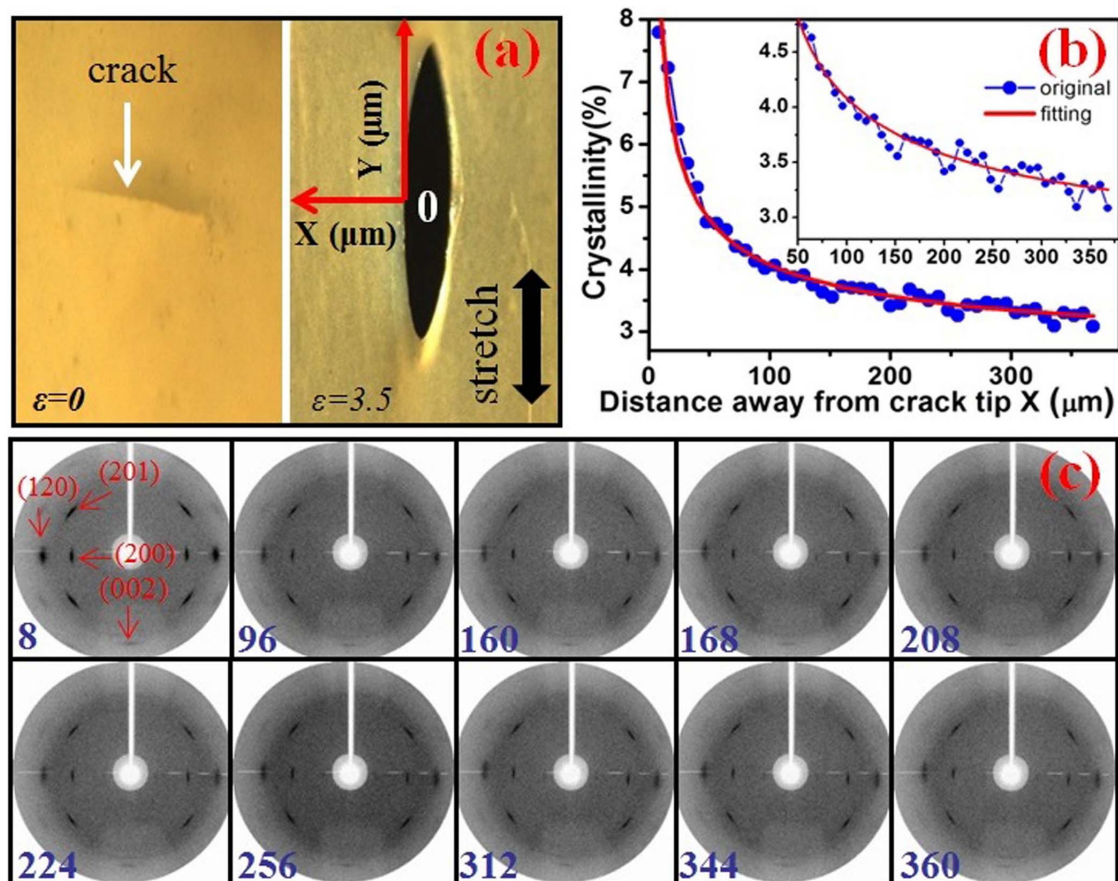


Figure 1 | (a) The photomicrograph of natural rubber film at $\varepsilon = 0$ and $\varepsilon = 3.5$, respectively; here a coordinate system is indicated by the arrows with X axis perpendicular to and Y axis parallel with the stretching direction. The zero point is located on the edge of the crack tip; (b) the crystallinity distribution in blue dots as a function of X and the fitting curve in red based on the Hook's law at $\varepsilon = 3.5$. The results suggests a decay trend of the crystallinity, coupled with weak oscillations as better observed by inserted curve for $X > 50$ μm ; (c) 2D SR- μSXRD diffraction patterns at selected positions in Figure 1 (b) with X values labeled in blue. The (200), (201), (120) and (002) planes can be found in the 2D diffractions as labeled in red words.

hierarchy in micro scale, the essential information in building theoretical toughening models to describe the mechanical enhancement mechanism²⁰. To shed a light on the physical pictures of the toughening mechanism of natural rubber, structural distribution with high spatial resolution in a larger area around the crack is crucial. In this study synchrotron radiation micro-beam scanning X-ray diffraction (SR- μSXRD) is employed to characterize *in-situ* the crystallinity distribution of cracked natural rubber under stretch, the high brilliance of which allows scan on a large area with relatively short time and detection of weak crystalline signal. By mapping the vicinity of crack tip of a pre-cut natural rubber film with focused X-ray of spot size about $5 \times 5 \mu\text{m}^2$, wide-angle X-ray diffraction patterns are measured and local crystallinity is derived at different locations for various strains. A two-dimensional (2D) oscillating pattern of crystallinity distribution is revealed under higher strain, indicates a network composed by alternating soft and hard regions or the so called double network structure. The formation of the double network structure enhances the toughness by 3 orders in comparison with homogeneous structure without network and can be attributed to interplay between crystallization and strain distribution.

Results

Figure 1 (a) shows two images of natural rubber samples with a pre-cut under strains of 0 and 3.5, respectively, showing deformation and enlargement of the crack along the stretching direction. Representative two-dimensional (2D) SR- μSXRD patterns mapped

at different selected distances away from the crack tip at $\varepsilon = 3.5$ are displayed in Figure 1 (c), which show crystalline diffraction points of natural rubber. The diffraction patterns indicate that all crystals orient along the stretching direction with a lateral sizes about 20 and 8 nm in (200) and (120) planes, respectively (Fig. S1 in Supplementary Information). Based on the 2D diffraction patterns, we calculate the crystallinity at each location. The distribution of calculated crystallinity along X axis is presented in Figure 1 (b), which gradually decays with increasing distance from the crack tip, similar to previous reports³¹. This decay trend may be fitted with stress distribution based on the formula³² with $\sigma \approx K/(2\pi r)^{0.5}$ as depicted by the red curve. Interestingly, weak oscillation of crystallinity is observed superposed on the fitting curve.

The 2D crystallinity distributions around the crack tip for samples stretched at different strains are presented in Figures 2 (a)–(d), which are extracted from thousands of diffraction patterns. Three features are observed from these 2D crystallinity distributions: (i) the overall crystallinity increases with the increase of strain; (ii) crystallinity follows a decay trend with increasing X; (iii) a 2D oscillation pattern is perceived from alternating blue and yellow colors in the 2D crystallinity distributions superposed on the decay trend. (i) and (ii) are consistent with the general expectation of strain-induced crystallization of natural rubber¹, where higher strain corresponds to higher crystallinity. Thanks to the high spatial resolution of SR- μSXRD , 2D oscillation of crystallinity around the crack tip is revealed, which may be the key structural origin for the excellent crack resistance. Clearly,

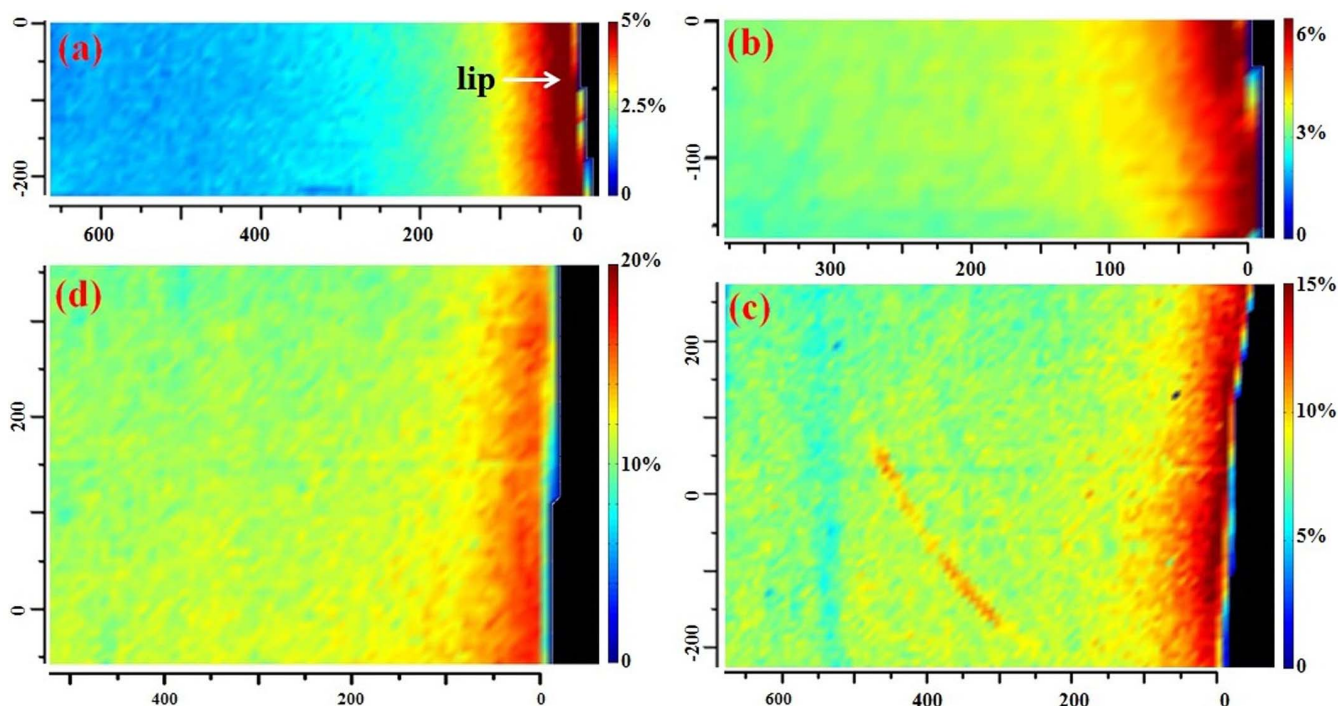


Figure 2 | The calculated 2D crystallinity distributions around the crack tip at different strains: (a) $\varepsilon = 3.0$; (b) $\varepsilon = 3.5$; (c) $\varepsilon = 4.5$; (d) $\varepsilon = 5.5$, which are extracted from 2,464; 1,000; 5,670 and 3,550 diffraction patterns, respectively. The transition of false color from red to blue indicates decrease of crystallinity with increasing distance away from the crack lip. However local oscillation of crystallinity can be perceived from alternating blue and yellow colors in the 2D crystallinity distributions, which can be interpreted as a double network structure composing of domains with high and low crystallinity. The red stripe in Figure 2 (c) distant from the lip does not influence the nearby oscillation pattern.

the 2D oscillation patterns represent a deformed double network structure composing of regions with high and low crystallinity, respectively. As high crystallinity corresponds to high modulus and vice versa, it represents a soft-hard double network structure, significantly increasing the crack resistance^{33,34}. Based on numerical statistics on Figure 2, the mesh sizes vary from 22 to 80 μm with averaged size along the long and short axis at about 45 and 35 μm , respectively (Fig. S3 and S4 in Supplementary Information). More obvious pattern after magnifying images in Figure 2 near and far away from the crack tip can be seen in Figure 3.

Based on the SR- μSXR D results above, we present in Figure 4 a schematic illustration of the evolving double network structure composed of hard and soft regions with different density of lamellae (crystallinity) near the crack tip. Domains with higher crystallinity tend to be harder and more difficult to be deformed. Upon stretching to a critical strain, at the region close to the crack tip, high crystallinity spots emerge out from the originally amorphous region due to strain induced crystallization and form a hard domain (see bottom part, Figure 4 (a)). The singular stress field at the crack tip can be alleviated through the coupled deformation between hard and soft

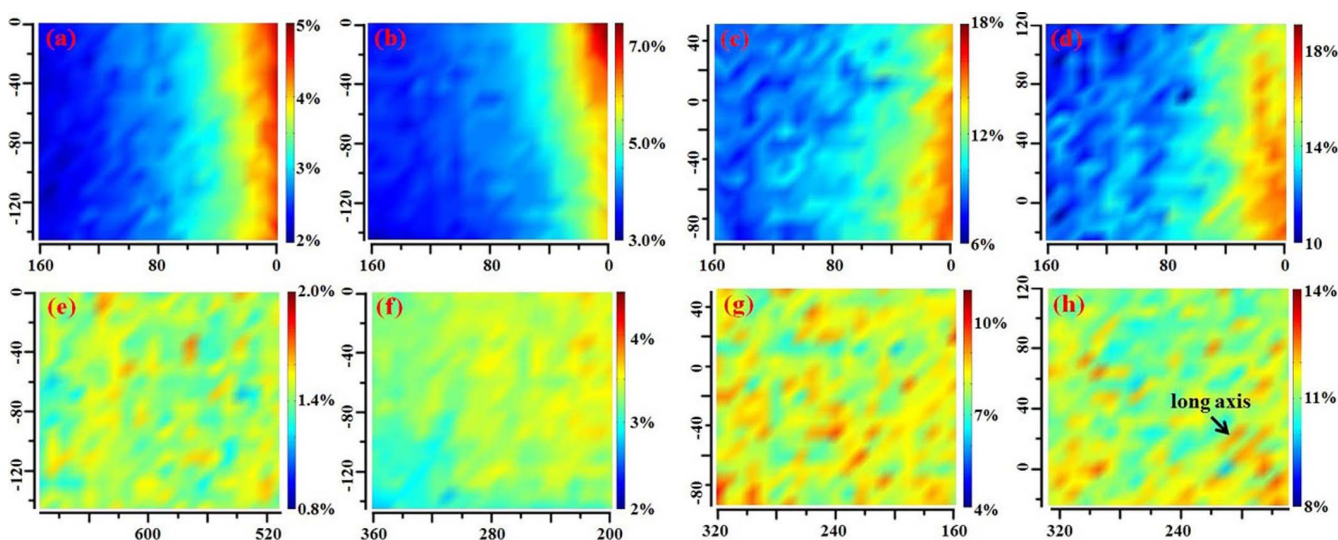


Figure 3 | The 2D local crystallinity distributions enlarged from Figure 2 in the vicinity of the crack tip ((a)–(d)) and far away from the crack tip ((e)–(h)) at different strains. From Figures 3. (a)–(d), the long axis of double network structure in the vicinity of the crack tip is roughly aligned to the stretching direction, while far away from the crack it tilts about 45° relative to the stretching direction obtained from Figures 3 (e)–(h).

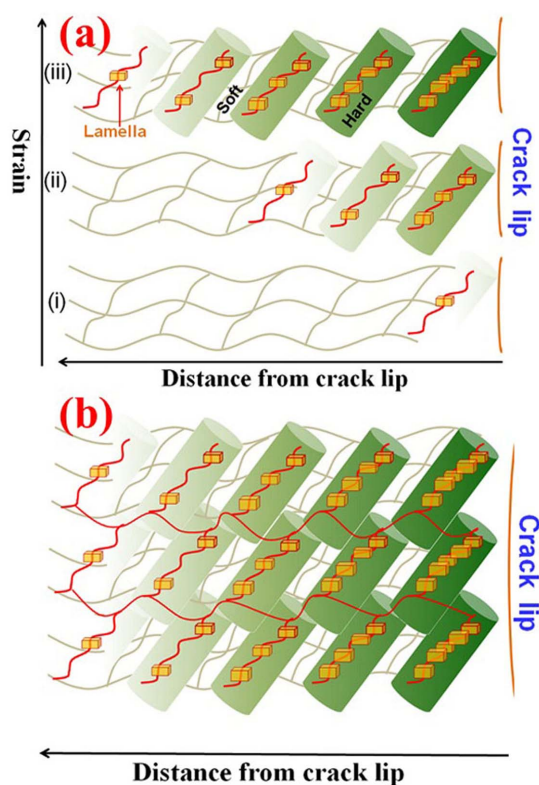


Figure 4 | A schematic illustration of the generation mechanism for the double network structure around the crack tip of stretched natural rubber, incorporating molecular conformational structure and nano-scale crystallization. Areas shaded in turquoise denote hard domains with higher crystallinity consisting of strain induced lamella. Random network in grey denote soft domains with lower crystallinity, where less amount of lamella may exist but are not shown for simplification. Bottom part (i) in panel (a) describes at low strain, the amorphous rubber chains are stretched as highlighted by red segment. The strain induced lamellae form a hard domain in the vicinity of the crack tip where local stress is concentrated as illustrated in part (ii). Upon formation of such hard domain which loads more stress, adjacent chains feel smaller effective stress and the crystallization is restrained, creating a relatively soft domain next to the original hard domains. As strain increases, crystallization occurs at locations even farther away and generates another hard domain; while the intercalated soft domain remain less hard or less crystallized, creating periodic structures as illustrated in part (iii). Panel (b) demonstrates how random shift during the formation of soft-hard patterns convert the one dimensional periodic structure into a deformed network structure. Thus the double network structure is generated through the cooperation of network structure of soft amorphous chains (in grey) and hard regions (in red).

domains. According to a simplified view from parallel model in classical mechanics of composite materials³⁵, soft and hard domains are stretched identically and hard domains bear most forces, which will hinder crystallization of the natural rubber chains between hard domains. As strain increases, the originally less stretched portion farther away from the tip is stretched to crystallize into new observable hard domain, and periodic arrangement of one dimensional texture with hard and soft domains goes up (middle and top part in Figure 4 (a)). Such a periodic structure attributed to the nonlinear response of stretched natural rubber is similar to the mechanism in most observed patterns in nature like the strips on zebra skin³⁶. Taking into account that a random shift will occur distant from the crack lip, the double network patterns observed by experiments can be obtained through stacking the one dimensional periodic tex-

ture as demonstrated in Figure 4(b). We can see from Figure 2 and 3 that the long axis direction of network structure of the hard regions away from the crack tip is obviously related to the principal direction which inclines about 45° to stretching direction because of the local stress field around the reoriented crack.

The shear lag model, commonly used to explain the enhancement mechanism for the hierarchical structure materials such as nacre and other bioinspired materials^{37–39}, can be applied to the current situation. The long intrinsic shear persistence length in the soft and hard double network structure leads to dispersing of the localized force into larger area and thus the force can be sustained by more cis-polyisoprene chains. Thus one can expect a substantial increase in fracture toughness, which account for the high crack resistance. Considering the morphology of the hard-soft double network structure shown in Figure 2 and 3, here we use the double network model developed by Okumura⁴⁰ instead of the shear lag model, for a better quantitative calculation of the toughening effect. The fracture energy ratio λ of the double network structure and homogeneous hard component structure is supposed to reflect the toughening effect of strain induced crystallization and defined as⁴⁰

$$\lambda \approx (1 - \phi_h) \frac{\zeta}{a_h} \frac{\mu_h}{\mu_s} \quad (1)$$

under the equal stress condition or

$$\lambda \approx \phi_h \frac{\zeta}{a_h} \quad (2)$$

under the equal strain condition. ϕ_h is the volume fraction of hard domains; ζ is the distance between adjacent hard domains; μ_h and μ_s are the elastic modulus for the hard and soft domains, respectively; a_h is the characteristic microscopic size of defect or Griffith cavities for the hard domains⁴¹. From equations (1)–(2), we see that an optimized value of ϕ_h can lead to maximal λ , otherwise structures of uniform hard ($\phi_h = 1$) or soft ($\phi_h = 0$) regions can only achieve the lowest value of $\lambda = 1$.

At the strain of 3.5, taking $\phi_h = 0.52$, $\mu_s = 2.96$ MPa, $\mu_h = 3.53$ MPa, $\zeta = 35$ μm , $a_h = 0.148$ μm (these parameters obtained at regions far from the crack tip in Figures 3 (e)–(h), see Supplementary Information), $G_c = 100$ J/m²⁴², we obtain $\lambda \approx 131$ from equation (1) under the equal stress condition, indicating that the double network structure enhances the crack resistance by 131 times than that of the homogeneous structure. Following similar approach, we calculate the enhancement factors (Figure 5 (a)) at different strains with two limit conditions defined by equations (1) and (2). We obtained that the factor λ reaches about 1,400 or 980 at strain 5.5 under the equal stress or equal strain condition, respectively. As discussed by Okumura⁴⁰, the enhanced toughness comes from a cut-off factor ζ/a_h and a modulus factor μ_h/μ_s (Figure 5 (b)). The former helps to spread stress to larger volume, while the later indicates the ability to store energy by soft domains. Larger value of either factor due to strain induced crystallization will improve the fracture toughness. Though parameters in our calculations derived from experimental data may vary with different areas, the enhancement effect of the double network structure is strikingly high, which can quantitatively explain the excellent crack resistance of natural rubber.

Toughening due to strain-induced crystallization in natural rubber has been well recognized since the dawn of rubber industry, which, however, is somehow restricted in the view of as-generated lamellas acting as in-situ hard filler. The hierarchy of natural rubber in the microscale seems to have been overlooked, which can be essential origin for high performance materials as inspired by other biopolymers like collagen and spider silk. Combing our findings of double network structure in microscale with the earlier pictures, the spontaneous multi-scale hierarchical structure of natural rubber emerges. The entropic elasticity stems from chain conformation at molecular level, taking a leading role at low strain; crystallization

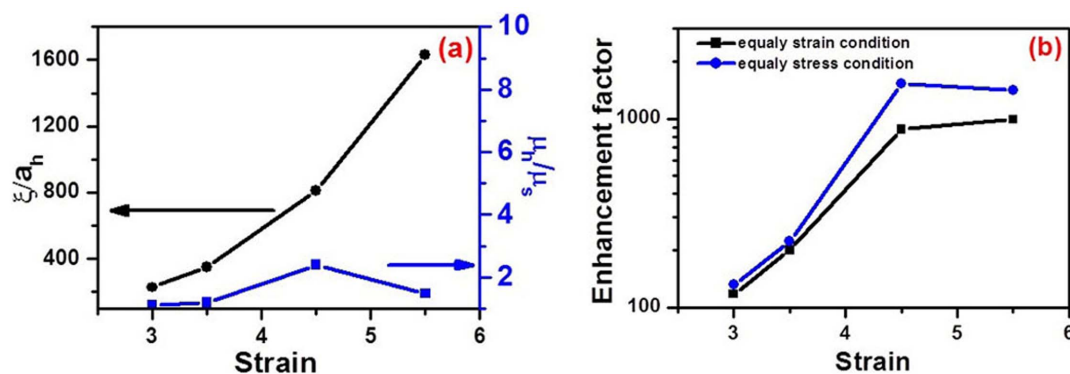


Figure 5 | (a) The relation between the cut-off factor ζ/a_h and modulus factor μ_h/μ_s with strain; (b) The relation between the enhancement factor λ with strain calculated in the framework of double network model using equation (1) under the equal stress condition and equation (2) under the equal strain condition. The cut-off factor rises up quickly with the strain increasing, indicating redistribution of local stress in larger areas. While the slower increment of modulus factor suggests slowly increasing of the ability to store energy by soft domains as strain increases. λ increases with the strain increasing and reaches about 1,400 or 980 at strain 5.5 under the equal stress or equal strain condition, respectively.

induced by strain in nanometer scale contributes an enthalpic elasticity at large strain⁴³; hard and soft double network structure amplifies the effect of strain-induced crystallization on reducing stress concentration through the cut-off factor ζ/a_h and on increasing the stored fracture energy through the modulus factor μ_h/μ_s in micro scale. The outstanding properties of natural rubber may come from the synergetic performance of the spontaneous hierarchy in these three length scales. Under external loading, the occurrence of crystallization in nanoscale is due to strain-induced conformational transition at molecular scale, which serves as a relay from entropic to enthalpic elasticity and prevents chain from fracturing. The interplay between crystallization and strain distribution leads to the formation of double network structure, which avoids stress concentration around the crack tip and fractures of crystals as well as molecular chains. The orchestrated coherence of the spontaneous hierarchical structure makes natural rubber as an intelligent and stimuli-responsible material with outstanding mechanical properties.

In summary, high spatial resolved SR- μ SXRD reveals that a soft and hard double network structure is created by strain-induced crystallization in the vicinity of crack tip, which leads to the formation of the multi-scale hierarchical structure in natural rubber. The emergence of double network structure is due to the interplay between crystallization and strain distribution, which enhances the fracture toughness by 3 orders of magnitude theoretically and explains the outstanding crack resistance of natural rubber. The coherence in these spontaneous multi-scale hierarchical structures, between conformation at molecular level, crystallization in nanoscale and the soft-hard double network structure in microscale, leads to the high toughness of natural rubber. Our discovery elucidates key structural

information responsible for the excellent resilience and resistance to fatigue crack propagation of natural rubber, bridging the gap between natural and synthetic rubbers. The proposed toughening mechanism integrating multi-scale dimensional elements from molecular level to microscale will not only stimulate further discussion leading to more refined and deeper understanding on this issue, but also promote analysis and optimization of natural rubber's performance in real application.

Methods

Materials. The raw material used is the ribbed smoked sheet (RSS) No.1 from Indonesia, which is purchased from Chinese Academy of Tropical Agricultural Science. The recipe and cure condition for preparation of the rubber sample are shown in Table 1. The raw material was masticated for 2 min using a heatable double-roll operated at $55 \pm 5^\circ\text{C}$, and then mixed with the vulcanizing additives without sulfur for 2 min, and afterwards with the sulfur was added with the mixing time for 1 min. In the end all the compounds were mixed for further 5 min. Furthermore, natural rubber compounds were vulcanized in an electrically heated hydraulic press at 143°C , and 15 MPa for 15 min to obtain the 180 μm -thickness film. The natural rubber samples were prepared into rectangular shaped specimens ($15 \times 3 \text{ mm}^2$) for homemade miniature tensile device testing.

Experimental section. The prepared rectangular natural rubber film with a crack (600 μm long and perpendicular to the stretching direction) was mounted between two clamps of a homemade miniature tensile device, and then stretched to assigned strain ε with a constant strain rate of 18%/min. Then the tensile device was put on the platform of BL15U1 in Shanghai Synchrotron Radiation Facility (SSRF), and the 2D crystallinity distribution around the crack tip at the assigned strain was obtained by SR- μ SXRD with mapping method. Data from the beam profile show that the area of the microspot was $5 \times 5 \mu\text{m}^2$ with a wavelength of 0.124 nm. At each detected point, the exposure time and data-readout time was 4 and 8 s respectively; scanning step of $8 \times 8 \mu\text{m}^2$ and filter of 3.1% was used to avoid the radiation damage. Based on above parameters, it took 12.2 hours to collect 5460 diffraction patterns to map the 2D crystallinity distribution of an area of $500 \times 700 \mu\text{m}^2$.

The method of crystallinity calculating, mechanical parameters for hard and soft domains, crystallite sizes and mesh sizes for different strains are presented in the Supplementary Information.

ingredients	Loading level (phr ^a)
natural rubber	100
Stearic acid	5
ZnO	2
accelerator TT ^b	0.5
accelerator DTD ^c	0.5
accelerator DM ^d	0.5
Sulfur	1
curing time ^e (min)	15

^aParts by weight per hundred parts rubber (phr).
^bTetramethylthiuram disulfide.
^c4,4'-Dithiodimorpholine.
^dN-Cyclohexyl-2-benzothiazolyl sulfenamide.
^ecure temperature was 143 °C.

- Katz, J. R. Röntgenspektrographische Untersuchungen am gedehnten Kautschuk und ihre mögliche Bedeutung für das Problem der Dehnungseigenschaften dieser Substanz. *Naturwissenschaften* **13**, 410–416 (1925).
- Fox, T. G., Flory, P. J. & Marshall, R. E. Thermodynamics of Crystallization in High Polymers. VI. Incipient Crystallization in Stretched Vulcanized Rubber. *J. Chem. Phys.* **17**, 704–706 (1949).
- Treloar, L. R. G. Rubbers and their Characteristics - Real and Ideal. *Nature* **155**, 441–444 (1945).
- Katzenberg, F., Heuwers, B. & Tiller, J. C. Superheated Rubber for Cold Storage. *Adv. Mater.* **23**, 1909–1911 (2011).
- Heuwers, B. *et al.* Shape-Memory Natural Rubber: An Exceptional Material for Strain and Energy Storage. *Macromol. Chem. Phys.* **214**, 912–923 (2013).
- Quitmann, D. *et al.* Solvent-Sensitive Reversible Stress-Response of Shape Memory Natural Rubber. *ACS Appl. Mater. Interfaces* **5**, 3504–3507 (2013).



7. Quitmann, D. *et al.* Environmental Memory of Polymer Networks under Stress. *Adv. Mater.* **26**, 3441–3444 (2014).
8. Heuwers, B. *et al.* Stress-Induced Stabilization of Crystals in Shape Memory Natural Rubber. *Macromol. Rapid. Commun.* **34**, 180–184 (2013).
9. Flory, P. J. Thermodynamics of Crystallization in High Polymers. I. Crystallization Induced by Stretching. *J. Chem. Phys.* **15**, 397–408 (1947).
10. Yeh, G. S. Y. Strain-induced crystallization I. Limiting extents of strain-induced nuclei. *Polym. Eng. Sci.* **16**, 138–144 (1976).
11. Yeh, G. S. Y. & Hong, K. Z. Strain-induced crystallization, Part III: Theory. *Polym. Eng. Sci.* **19**, 395–400 (1979).
12. Tosaka, M. *et al.* Orientation and crystallization of natural rubber network as revealed by WAXD using synchrotron radiation. *Macromolecules* **37**, 3299–3309 (2004).
13. Toki, S. *et al.* Probing the nature of strain-induced crystallization in polyisoprene rubber by combined thermomechanical and in situ X-ray diffraction techniques. *Macromolecules* **38**, 7064–7073 (2005).
14. Che, J. *et al.* Crystal and Crystallites Structure of Natural Rubber and Synthetic cis-1,4-Polyisoprene by a New Two Dimensional Wide Angle X-ray Diffraction Simulation Method. I. Strain-Induced Crystallization. *Macromolecules* **46**, 4520–4528 (2013).
15. Che, J. *et al.* Crystal and Crystallites Structure of Natural Rubber and Peroxide-Vulcanized Natural Rubber by a Two-Dimensional Wide-Angle X-ray Diffraction Simulation Method. II. Strain-Induced Crystallization versus Temperature-Induced Crystallization. *Macromolecules* **46**, 9712–9721 (2013).
16. Toki, S., Hsiao, B. S., Amnuaypornsi, S. & Sakdapipanch, J. New insights into the relationship between network structure and strain-induced crystallization in unvulcanized and vulcanized natural rubber by synchrotron X-ray diffraction. *Polymer* **50**, 2142–2148 (2009).
17. Ikeda, Y. *et al.* Comparative study on strain-induced crystallization behavior of peroxide cross-linked and sulfur cross-linked natural rubber. *Macromolecules* **41**, 5876–5884 (2008).
18. Tosaka, M. *et al.* Effect of Network-Chain Length on Strain-Induced Crystallization of NR and IR Vulcanizates. *Rubber Chem. Technol.* **77**, 711–723 (2004).
19. Tosaka, M. *et al.* Crystallization and Stress Relaxation in Highly Stretched Samples of Natural Rubber and Its Synthetic Analogue. *Macromolecules* **39**, 5100–5105 (2006).
20. Le Cam, J. B. & Toussaint, E. The Mechanism of Fatigue Crack Growth in Rubbers under Severe Loading: the Effect of Stress-Induced Crystallization. *Macromolecules* **43**, 4708–4714 (2010).
21. Zhang, H. P. *et al.* Toughening effect of strain-induced crystallites in natural rubber. *Phys. Rev. Lett.* **102**, 245503 (2009).
22. Trabelsi, S., Albouy, P. A. & Rault, J. Crystallization and Melting Processes in Vulcanized Stretched Natural Rubber. *Macromolecules* **36**, 7624–7639 (2003).
23. Rublon, P. *et al.* In situ synchrotron wide-angle X-ray diffraction investigation of fatigue cracks in natural rubber. *J. Synchrotron Rad.* **20**, 105–109 (2013).
24. Tang, Z., Kotov, N. A., Magonov, S. & Ozturk, B. Nanostructured artificial nacre. *Nat. Mater.* **2**, 413–418 (2003).
25. Meyers, M. A., McKittrick, J. & Chen, P.-Y. Structural Biological Materials: Critical Mechanics-Materials Connections. *Science* **339**, 773–779 (2013).
26. Silva, L. P. & Rech, E. L. Unravelling the biodiversity of nanoscale signatures of spider silk fibres. *Nat. Commun.* **4**, 3014 (2013).
27. Rensberger, J. M. & Watabe, M. Fine structure of bone in dinosaurs, birds and mammals. *Nature* **406**, 619–622 (2000).
28. Peterlik, H., Roschger, P., Klaushofer, K. & Fratzl, P. From brittle to ductile fracture of bone. *Nat. Mater.* **5**, 52–55 (2006).
29. Kimata, S. *et al.* Molecular Basis of the Shish-Kebab Morphology in Polymer Crystallization. *Science* **316**, 1014–1017 (2007).
30. Bonderer, L. J., Studart, A. R. & Gauckler, L. J. Bioinspired Design and Assembly of Platelet Reinforced Polymer Films. *Science* **319**, 1069–1073 (2008).
31. Trabelsi, S., Albouy, P. A. & Rault, J. Stress-Induced Crystallization around a Crack Tip in Natural Rubber. *Macromolecules* **35**, 10054–10061 (2002).
32. Sadd, M. H. *Elasticity: Theory, Applications, and Numerics*. 275–277 (Butterworth-Heinemann, Oxford, 2005).
33. Sun, J.-Y. *et al.* Highly stretchable and tough hydrogels. *Nature* **489**, 133–136 (2012).
34. Gong, J. P., Katsuyama, Y., Kurokawa, T. & Osada, Y. Double-Network Hydrogels with Extremely High Mechanical Strength. *Adv. Mater.* **15**, 1155–1158 (2003).
35. Sendekyj, G. P. *Composite Materials*. Vol. 2, 46–53 (Academic Press, New York, 1974).
36. Gravan, C. P. & Lahoz-Beltra, R. Evolving morphogenetic fields in the zebra skin pattern based on Turing's morphogen hypothesis. *Int. J. Appl. Math. Comput. Sci.* **14**, 351–361 (2004).
37. Munch, E. *et al.* Tough, Bio-Inspired Hybrid Materials. *Science* **322**, 1516–1520 (2008).
38. Bouville, F. *et al.* Strong, tough and stiff bioinspired ceramics from brittle constituents. *Nat. Mater.* **13**, 508–514 (2014).
39. Ritchie, R. O. The conflicts between strength and toughness. *Nat. Mater.* **10**, 817–822 (2011).
40. Okumura, K. Toughness of double elastic networks. *EPL* **67**, 470–476 (2004).
41. Lawn, B. R. *Fracture of brittle solids 2nd ed.* 328–331 (Cambridge University Press, New York, 1993).
42. Gent, A. & Wang, C. Fracture mechanics and cavitation in rubber-like solids. *J. Mater. Sci.* **26**, 3392–3395 (1991).
43. Miserez, A., ScottWasko, S., Carpenter, C. F. & Waite, J. H. Non-entropic and reversible long-range deformation of an encapsulating bioelastomer. *Nat. Mater.* **8**, 910–916 (2009).

Acknowledgments

This work is supported by the National Natural Science Foundation of China (51325301, 51033004, 51227801, U1232128, 11272303, 51473151), 973 program of MOST (2010CB934504), fund for one hundred talent scientist of CAS, the Project 2013BB05 supported by NPL, CAEP. The experiment is carried out in SSRF (BL15U1 and BL16B1).

Author contributions

W.M.Z., L.B.L. and H.Y.L. designed the research and interpreted the results. W.M.Z. conducted the experiment with SR- μ SXRD and WAXS in SSRF, L.C. and Z.M.Q. assisted with the SR- μ SXRD experiment. J.L. developed a method to analyze the data. H.Y.L. contributed to the discussion of results. X.Y.L. and N.D.H. assisted with the manuscript writing. All authors commented on the manuscript.

Additional information

Supplementary information accompanies this paper at <http://www.nature.com/scientificreports>

Competing financial interests: The authors declare no competing financial interests.

How to cite this article: Zhou, W. *et al.* Toughening mystery of natural rubber deciphered by double network incorporating hierarchical structures. *Sci. Rep.* **4**, 7502; DOI:10.1038/srep07502 (2014).



This work is licensed under a Creative Commons Attribution-NonCommercial-ShareAlike 4.0 International License. The images or other third party material in this article are included in the article's Creative Commons license, unless indicated otherwise in the credit line; if the material is not included under the Creative Commons license, users will need to obtain permission from the license holder in order to reproduce the material. To view a copy of this license, visit <http://creativecommons.org/licenses/by-nc-sa/4.0/>